

Flubendazole: New Corrosion Inhibitor for 6061Al-Si Alloy in 0.1M HCl Medium

A. S. Fouda^{1,*}, F.I. El-Dossoki², W.T.Elbehairy¹, A.Elmoahady¹

¹ Department of Chemistry, Faculty of Science, El-Mansoura University, El-Mansoura-35516, Egypt,

² Department of Chemistry, Faculty of Science, Port Said University, Egypt

*E-mail: asfouda@hotmail.com, asfouda@mans.edu.eg

Received: 9 July 2018 / Accepted: 11 September 2018 / Published: 1 October 2018

The inhibition performance of Flubendazole (FBZ) drug on the corrosion of the 6061Al-Si alloy in 0.1M HCl has been observed by AC impedance (EIS), Tafel diagrams, electrochemical frequency modulation (EFM) and mass loss (ML) methods. The inhibition efficiency (IE) rises by raising the Flubendazole extent (FBZ) and diminished by raising the temperature. Polarization curves have shown that the Flubendazole acts as a mixed-kind inhibitor. FBZ adsorption on the alloy surface was obeying Temkin isotherm. Thermodynamic adsorption functions (ΔG°_{ads} , ΔH°_{ads} and ΔS°_{ads}) and the activation parameters (E^*_a , ΔH^* , ΔS^*) were calculated and analyzed. Surface analysis using Scanning Electron Microscopy (SEM) has confirmed the existence of a protective film of drug molecules onto Al alloy surface. The surface analysis of Al alloy was performed by scanning electron microscope (SEM), AFM (atomic force microscopy) and (FT-IR) Fourier transform infrared spectra.

Keywords: Corrosion, Adsorption, Al alloy, HCl, SEM, AFM, FTIR

1. INTRODUCTION

Aluminum is used in several industrial and engineering applications as a result of its cost effectiveness and excellent properties. Therefore, Aluminum and its alloys are used in various environments containing acids, alkalis and salt solutions where they undergo corrosive attacks [1]. The most effective and practical method to decrease corrosion processes is the addition of inhibitors to the metal's environment. Foregoing studies showed that heterocyclic compounds are employed as corrosion inhibitors because of the presence of a number of active centers (O, N, S, P, and π electrons) which can form a protective thin film on a metal [2]. Drugs are a better choice due to the fact that they are environmentally nonthreatening and contain amazingly amusing source of naturally synthesized organic compounds. The choice of some drugs used as corrosion inhibitors is based on the following

justifications: (a) drugs are mainly soluble in aqueous media, (b) drug molecules contain O, N and S as donatin centers, (c) drugs are non-polluted and (d) drugs can be easily synthesized [3-6]. Some drugs were reported in the literature as effective corrosion inhibitors in acidic media such as: streptomycin [7], sulfacetamide [8,9], sulfadiazine and sulfamethazine [10], rhodanine [11], orphenadrine [12], sparfloxacin [13], cefazolin [14], trimethoprim [15], cefepime and cefoperazone [16], tramadol [17], cefalexin [18], cefixime [19], mebendazole [20], cefadroxil [21], ciprofloxacin, norfloxacin and ofloxacin [22].

The current study reports the performance of Flubendazole, the objective of this research is to examine the inhibiting behavior of Flubendazole on the corrosion of Al-Si alloy in 0.1 M HCl utilized chemicals and electrochemical tests. The sample surface analyses were also analyzed.

2. MATERIALS AND TECHNIQUES

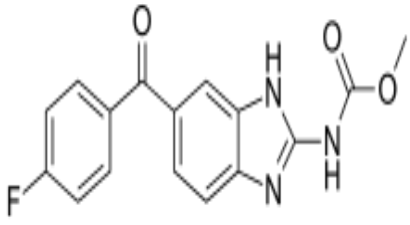
2.1. Materials and solutions

The metal sample conformation in weight % is: Si 0.67, Fe 0.19, Cu 0.24, Mn 0.01, Mg 1.00, Cr 0.05, Zn 0.01, Ti 0.02 and Al the rest

2.2. Inhibitor

Table 1 describes the Flubendazole (FBZ) structure.

Table 1. Chemical assemblies of the FBZ

Structure	IUPAC Name	Molecular weight
 <p style="text-align: center;">C₁₆H₁₂FN₃O₃</p>	Methyl N-[6-(4-fluorobenzoyl)-1H-benzimidazol-2-yl] carbamate	313.28 g/mol

2.3. Chemicals and solutions

Al-Si alloy specimens were used. The aggressive medium used is HCl 37%. Solutions of 0.1 M HCl were prepared by dilution with distilled water. The Flubendazole stock solution 10³ ppm was used to prepare (50, 100, 150, 200, 250 and 300 ppm).

2.4. Methods

2.4.1. Mass loss (ML) technique

The coins with size ($2 \times 2 \times 0.2$ cm) x2 were dipping in 0.1M HCl (100 ml) and with (50-300ppm) of FBZ are set in water thermostat. After 3 h the samples were removed, rinsed, dried, and weighed again. The % IE and the θ were founded by (1):

$$\% \text{ IE} = \theta \times 100 = [(W^{\circ} - W) / W^{\circ}] \times 100 \quad (1)$$

Where W° and W are the weights of nonexistence and occurrence of FBZ, individually.

2.4.2. Potentiodynamic polarization (PP) technique

This technique was done in a typical three compartment glass cell. The potential range was (-1.0 to -0.6V vs. SCE) at OCP with a scan rate 1 mVs^{-1} .

2.4.3. EIS technique

This technique was done by AC signs of 5 mV peak to peak amplitude and at frequency range of 10^7 Hz to 0.1 Hz. The (% IE) and θ were founded from eq. (2) [23]:

$$\% \text{ IE} = 100 \times \theta = 100 \times [(R_{ct} - R_{ct}^{\circ}) / R_{ct}] \quad (2)$$

Where, R_{ct}° and R_{ct} are the charge transfer resistances without and with FBZ, individually.

2.4.4- EFM test

This technique used two frequencies of range 2 and 5 Hz depended on three conditions [24]. The (i_{corr}), (β_c and β_a) and (CF-2, CF-3) (Causality factors) were measure by the greater two peaks [25].

2.4.5. Surface examinations

Al alloy pieces were dipped in testing solutions for one day. Then, they were polished, dried and analyzed by (SEM), (FTIR) and (AFM).

3. RESULTS AND DISCUSSION

3.1. Potentiodynamic polarization (PP) tests

Tafel curves of Al alloy electrode in 0.1M HCl with and without various contents of Flubendazole can be studied from Figure 1. From Table 2 FBZ has effect on both of cathodic and anodic processes and the IE rises with rise of the FBZ content. E_{corr} was a little changed, indicating that FBZ acts as a mixed-kind inhibitor. i_{corr} reduced through the FBZ addition to 0.1M HCl. % IE and (θ) were found from eq. (3):

$$\% IE = \theta \times 100 = [(i_{corr} - i_{corr(inh)}) / i_{corr}] \times 100 \tag{3}$$

Where, i_{corr} is the current density in absence of FBZ and i_{corr} in presence of FBZ.

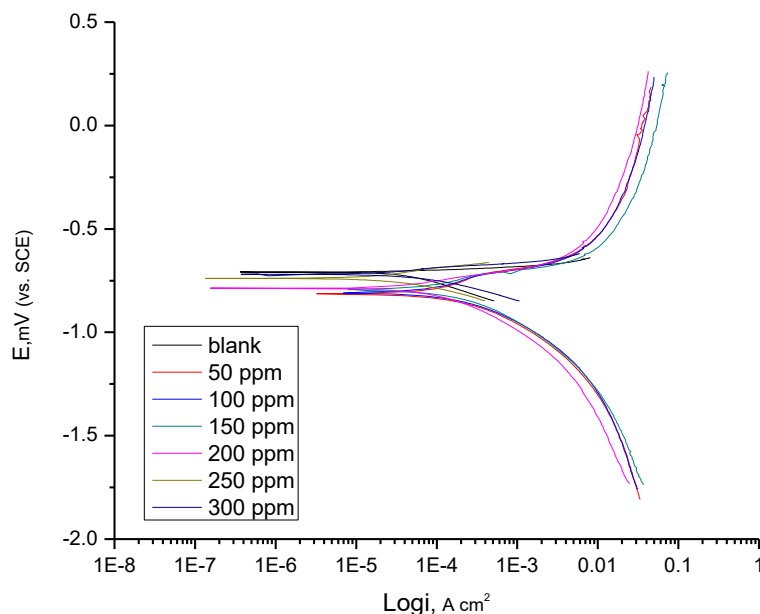


Figure 1. Polarization curves of the Al alloy dissolution with and without different concentrations of Flubendazole at 25°C

Table 2. PP results of Al alloy dissolution with and without different concentrations of FBZ at 25°C

Conc., ppm	i_{corr} , $\mu A\ cm^{-2}$	$- E_{corr}$, mV vs SCE	β_a , mV dec ⁻¹	β_c , mV dec ⁻¹	C.R mpy	Θ	% IE
0	22.1	709	15.8	79.1	31.6	-----	-----
50	18.5	714	187.9	223.9	7.9	0.163	16.3
100	17.6	708	150.4	240.4	7.6	0.204	20.4
150	15.9	693	119.1	241.8	6.8	0.281	28.1
200	10.2	686	105.5	230.7	4.4	0.538	53.8
250	5.6	739	331.0	113.7	4.2	0.747	74.7
300	2.8	719	211.9	235.1	4.0	0.873	87.3

3.2. (EIS) tests

From Figure 2 the semi-circle diameter was raised by increasing of FBZ concentration. Figure 3 indicates the utilizing circuit for fitting the gotten results [26]. The C_{dl} and Y^0 were founded from eq. (4) [27]:

$$C_{dl} = Y^0 \omega^{n-1} / \sin [n (\pi/2)] \tag{4}$$

where $\omega = 2\pi f_{max}$, f_{max} is the greater frequency and n is the exponential. R_{ct} increases with the rise of the double layer thickness [28]. From Table 3, the C_{dl} decline as a result of the replacement of adsorbed water molecules by FBZ species [29]. These results prove the occurrence of a protective adsorbed layer.

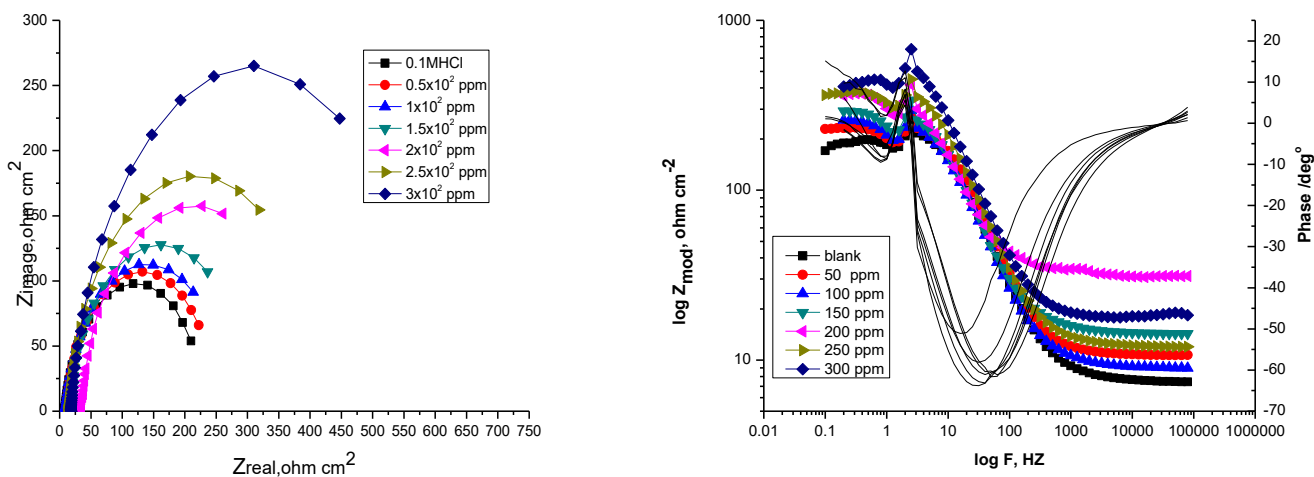


Figure 2. EIS Bode and Nyquist curves for Al-Si alloy in 0.1M HCl with and without various concentrations of FBZ drug at 25°C

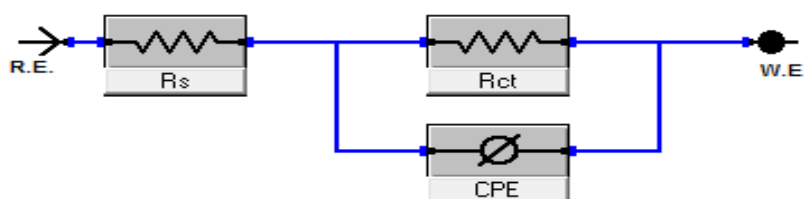


Figure 3. Circuit utilized for fitting the EIS data in 0.1M HCl

Table3. EIS parameters for the tested alloy without and with different concentrations of FBZ at 25°C

Conc., ppm	R_{ct} , $\Omega \text{ cm}^2$	C_{dl} , $\mu\text{F cm}^{-2}$	θ	%IE
Blank	142.2	177.1	----	----
50	215.1	92.2	0.339	33.9
100	232.0	81.3	0.387	38.7
150	256.7	80.9	0.446	44.6
200	303.7	64.0	0.532	53.2
250	354.0	60.9	0.598	59.8
300	423.5	49.6	0.664	66.4

3.3. (EFM) tests

EFM is characterized by speed and greatly accuracy in calculating the current data [30]. Figure 4 indicates the EFM of Al-Si alloy in 0.1M HCl solution and 300 ppm of FBZ. The EFM parameters such as (CF-2 and CF-3), (β_c and β_a) and (i_{corr}) can be measured from the higher current peaks. The CF is closer to the standard data proved the validity of the calculated data. The IE% increase with the raising of FBZ concentrations. From table (4), the addition of FBZ with different concentrations to the corrosive medium reduces the current density of corrosion, meaning that drug act as inhibitor by adsorption process.

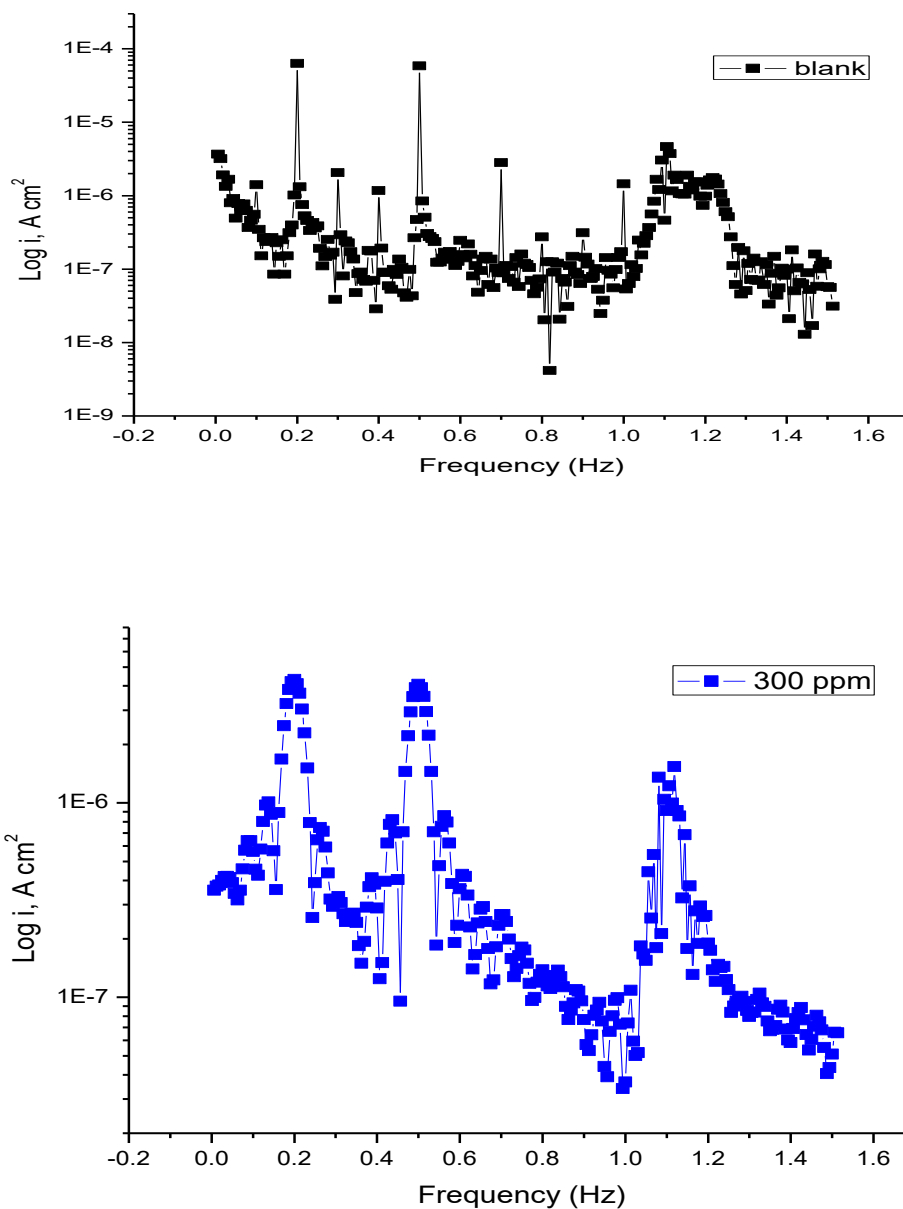


Figure 4. EFM diagrams for Al-Si alloy in 0.1M HCl and 300 ppm from FBZ at 25°C

Table 4. Parameters of EFM diagrams for Al-Si alloy in absence and presence of various concentrations of FBZ in 0.1M HCl at 25°C

Conc., ppm	i_{corr} $\mu\text{A cm}^{-2}$	β_c , mV dec^{-1}	β_a , mV dec^{-1}	C.R, mpy	CF-2	CF-3	Θ	%IE
0	99.9	123	95	142.9	1.9	2.9	---	---
50	69.5	133	117	99.4	1.6	2.7	0.304	30.4
100	69.4	147	105	97.6	2.1	3.2	0.305	30.5
150	69.3	150	131	97.3	1.9	3.3	0.306	30.6
200	66.4	114	84	85.9	1.7	3.2	0.335	33.5
250	52.8	150	93	84.4	1.5	3.3	0.471	47.1
300	19.3	83	77	82.6	1.3	2.7	0.806	80.6

3.4. Mass loss (ML) tests

The reduction in mass of Al alloy can be studied in occurrence of FBZ at 30°C. Figure 5 shows that FBZ decreases the mass reduction and therefore corrosion rate. The (%IE) and then θ , of the FBZ for the Al alloy were founded by eq. (1) [31]. The values of %IE are given in Table 5.

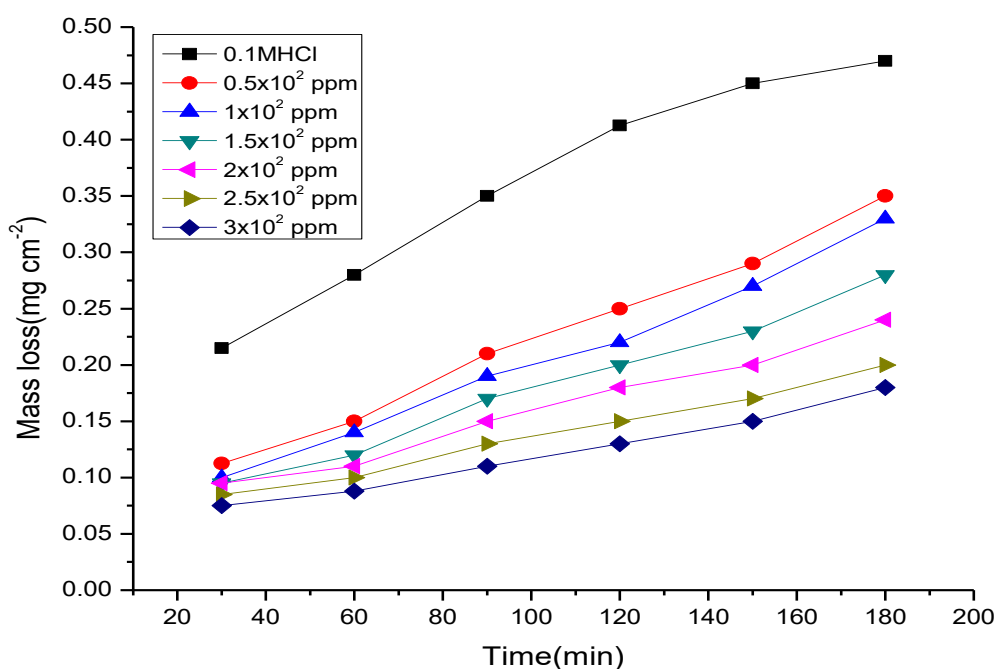


Figure 5. Mass loss-time relationship of Al-Si alloy corrosion in absence and presence of various concentrations of FBZ at 25°C

Table 5. Values of IE after 120 min of Al-Si alloy in absence and presence of FBZ concentrations of at 25°C

Conc., ppm	FBZ drug	
	% IE	Θ
50	30.4	0.304
100	45.7	0.457
150	60.0	0.600
200	72.6	0.726
250	78.7	0.787
300	87.2	0.872

3.5. Influence of temperature

The results of Table 6 indicate that %IE was reduced with rising of temperature. The decrease in % IE with the rising of the temperature proved the presence of physical adsorption of FBZ drug.

Table 6. Parameters such as %IE, (Θ) and (C.R.) for Al alloy dissolution after 120 min with and without various concentrations of FBZ drug at different temperatures

Conc., ppm	Temp, K	C.R., $\text{mg cm}^{-2} \text{min}^{-1}$	Θ	%IE
0.1MHCl	303	3.2	-----	-----
50		2.3	0.304	30.4
100		1.8	0.457	45.7
150		1.4	0.600	60.00
200		1.1	0.726	72.6
250		1.0	0.787	78.7
300		0.8	0.872	87.2
Blank	308	3.4	----	-----
50		2.4	0.203	20.3
100		1.9	0.376	37.6
150		1.5	0.485	48.5
200		1.2	0.564	56.4
250		1.1	0.639	63.9
300		0.9	0.685	68.5
Blank	313	3.5	----	-----
50		2.8	0.116	11.6
100		2.5	0.205	20.5
150		2.3	0.276	27.6
200		2.1	0.353	35.3

250	318	1.9	0.41	41
300		1.7	0.462	46.2
Blank		3.6	-----	-----
50		3.0	0.083	8.3
100		2.7	0.163	16.3
150		2.5	0.224	22.4
200	323	2.3	0.292	29.2
250		2.1	0.352	35.2
300		1.9	0.402	40.2
Blank		3.9	-----	-----
50		3.4	0.043	4.3
100		3.2	0.105	10.5
150	323	3.0	0.158	15.8
200		2.8	0.211	21.1
250		2.7	0.256	25.6
300		2.5	0.315	31.5

The equation of Arrhenius (6) can be used to measure the activation energy (E_a^*) of the activated complex [32]:

$$C.R. = A \exp(-E_a^* / RT) \tag{5}$$

where E_a^* is activation energy and T is the absolute temperature. Using Figure 6, E_a^* can be measured (Table 7). E_a^* values prove that the higher extents of FBZ impede corrosion effectively by raising the energy barrier of the activated complex and improve that the process is controlled by diffusion [33].

(ΔH^* , ΔS^*) are measured by (6) [34]:

$$C.R. = RT/Nh \exp(\Delta S^*/R) \exp(-\Delta H^*/RT) \tag{6}$$

Figure 7 describes the relation between $\log(C.R./T)$ and $(1/T)$ which used to measure the values of ΔH^* and ΔS^* (Table 7).

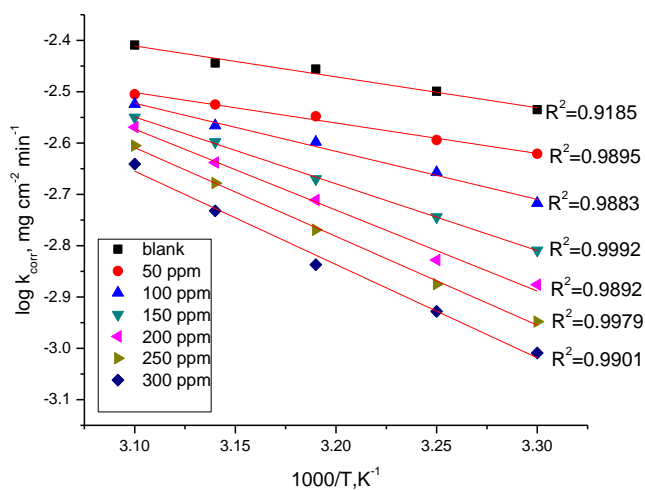


Figure 6. Log k_{corr} vs reciprocal of temperature plot for Al alloy in absence and presence of FBZ concentrations

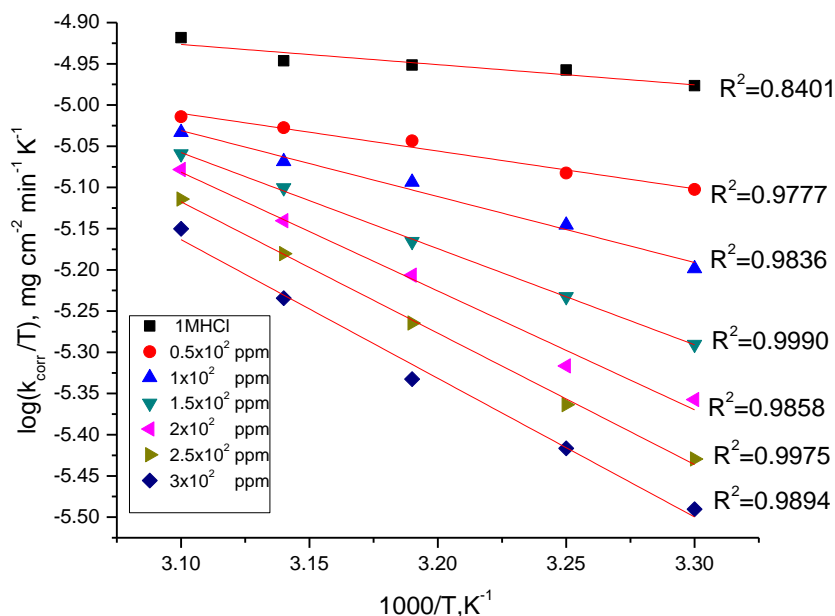


Figure 7. The relation between $\log C.R. / T$ and $1/ T$ diagrams for the Al alloy without and with several FBZ concentrations

In the chemisorption process, enthalpy must be or more than 100 kJ mol^{-1} [35]. The rise in the (ΔH^*) with the occurrence of the FBZ reflects the rise in the energy barrier of the corrosion procedures. The negative values of ΔS^* shows that during the rate-determining step in the formation of activated complex is highly frequent than the cracking [36].

Table 7. Data of activation for Al alloy without and with various concentrations of FBZ

Conc., ppm	E_a^* , kJ mol^{-1}	ΔH^* , kJ mol^{-1}	$-\Delta S^*$, $\text{J mol}^{-1}\text{K}^{-1}$
Blank	7.3	4.7	277.2
50	15.2	8.8	266.2
100	17.9	15.3	246.3
150	24.9	22.3	225.1
200	30.1	27.6	209.2
250	33.1	30.5	200.8
300	34.8	32.2	196.5

3.7. Adsorption isotherms

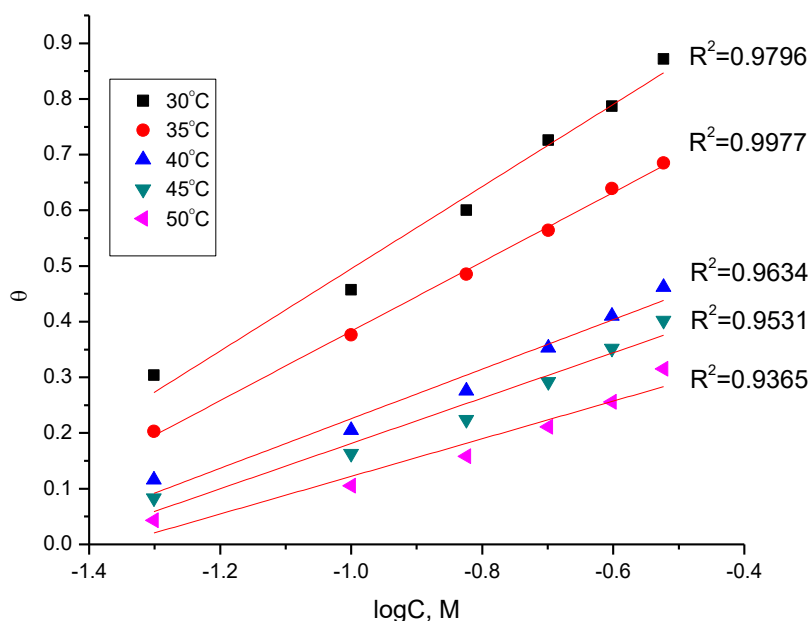


Figure 8. Temkin isotherm for the FBZ drug on Al alloy in 0.1 M HCl

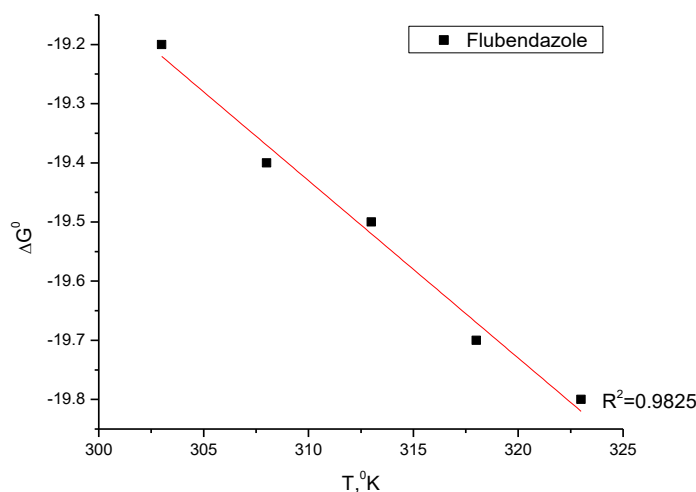


Figure 9. Plots ΔG°_{ads} vs T for the FBZ adsorption in 0.1M HCl

Figure 8 represented the Temkin isotherm, which used to calculate Θ values for FBZ. The Temkin equation represented as follows [37].

$$\Theta_{coverage} = (2.303/a) \text{Log } K_{ads} + (2.303/a) \text{Log } C \tag{7}$$

Where K_{ads} is the adsorption constant and C is the FBZ content (M).

The ΔG°_{ads} and K_{ads} data are in Table 8. The ΔG°_{ads} founded by:

$$\Delta G^{\circ}_{ads} = - RT \ln (55.5 K_{ads}) \tag{8}$$

The FBZ adsorption is spontaneous and this is proven by the ΔG°_{ads} negative sign. From the data of ΔG°_{ads} (around to -20 kJ mol^{-1}), proven that the FBZ adsorption is physisorption [38].

Vant't Hoff equation can be used to measure ΔH°_{ads} and ΔS°_{ads} [39] expressed by:

$$\ln K_{ads} = \frac{-\Delta H^{\circ}_{ads}}{RT} + const \tag{9}$$

And eq. (10):

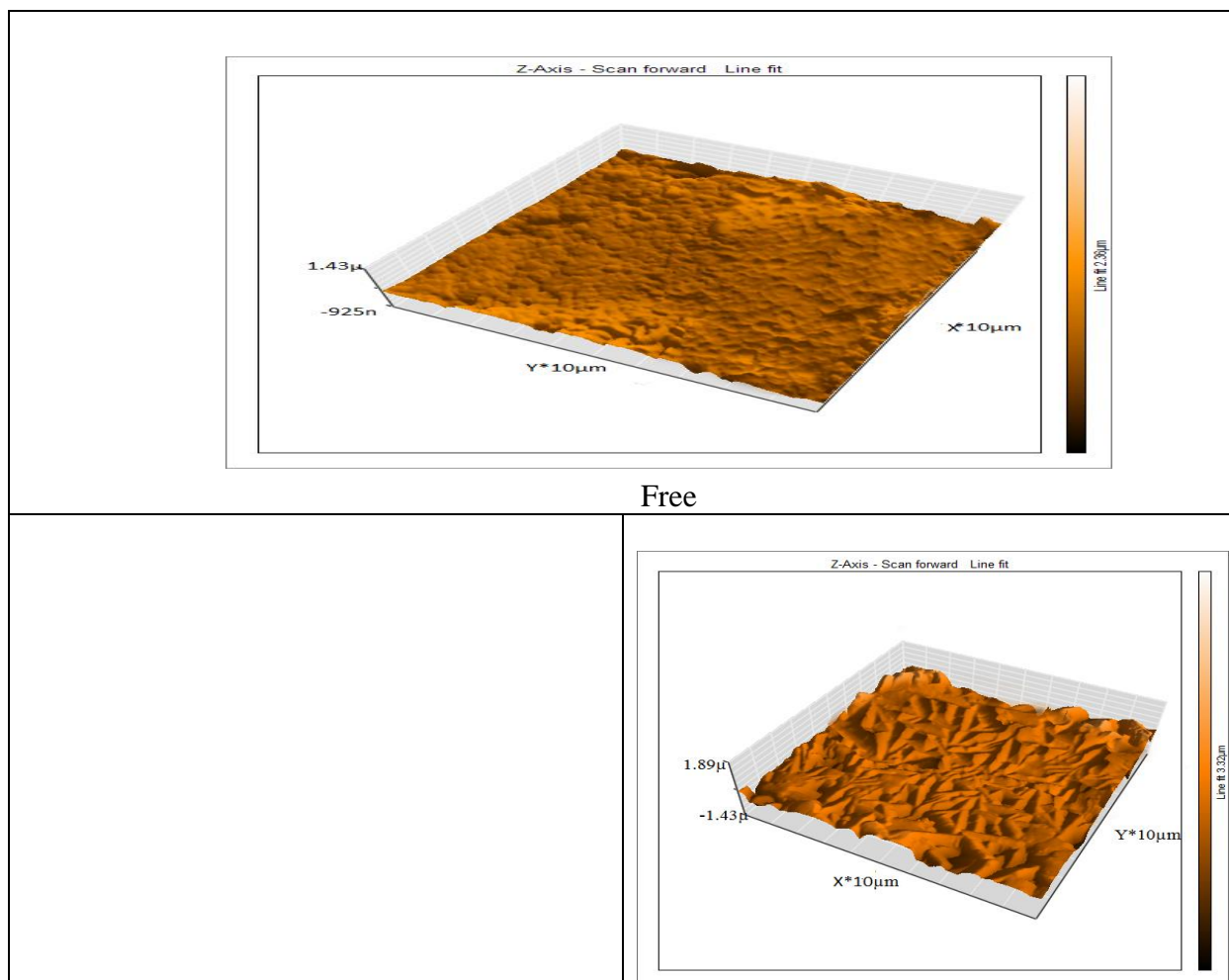
$$\Delta G^{\circ}_{ads} = \Delta H^{\circ}_{ads} - T \Delta S^{\circ}_{ads} \tag{10}$$

Figure 9 shows the relation between ΔG°_{ads} and T. A negative sign of ΔS°_{ads} proved that the disorder of corrosion process is decreases by using FBZ (Table 8) [40].

Table 8. Temkin data of Al alloy in absence and presence of various concentrations of FBZ at (30°C-50°C)

Temp., K	K_{ads} M^{-1}	$-\Delta G^{\circ}_{ads}$ $kJ\ mol^{-1}$	$-\Delta H^{\circ}_{ads}$ $kJ\ mol^{-1}$	$-\Delta S^{\circ}_{ads}$ $J\ mol^{-1}K^{-1}$
303	46.8	19.2	10.1	30
308	40.7	19.4		30
313	32.4	19.5		30
318	28.2	19.7		30
323	22.9	19.8		30

3.8. (AFM) analysis



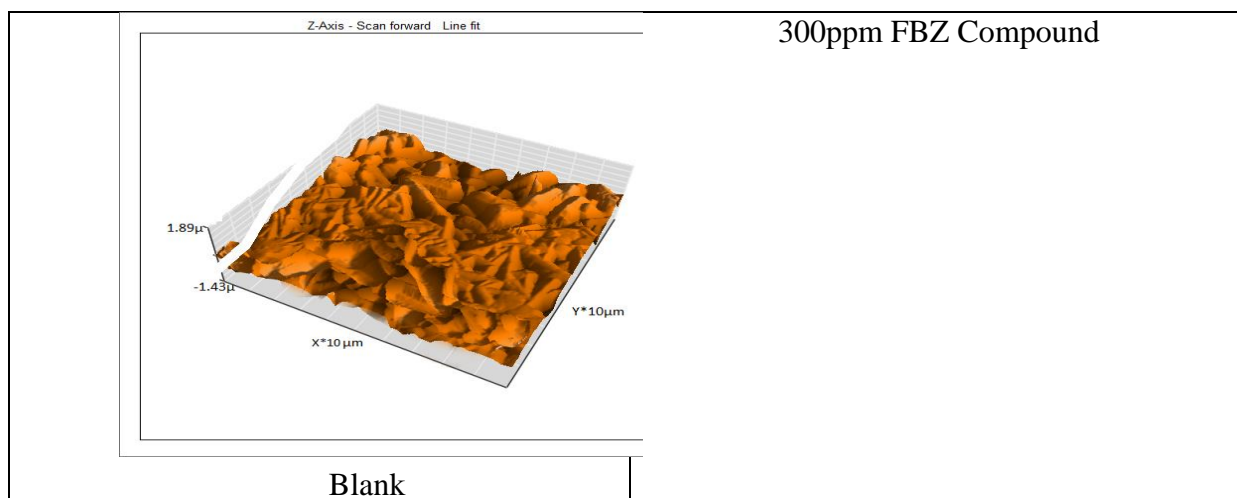


Figure10. (3D) AFM images of 6061 Al-Si alloy without acid (free), Al alloy in 0.1M HCl (blank), and Al alloy in 0.1 M HCl at 300 ppm of FBZ for 24 hours at 25°C

This method gives a map about the metal surface where roughness is indicated with an excessive resolve [41]. The 3D images of AFM shown in Figure 10.

Table 9. AFM parameters for 6061 Al alloy (a) pure coin (b) with for 24 hours (c) with corrosive medium containing 300 ppm FBZ for 24 hours

Parameters	A	B	C
The roughness average (Sa)	48.6	391.8	98.6
The mean value (Sm)	-16.6	-18.7	-16.6
The root mean square (Sq)	125.0	471.8	125.0
The valley depth (Sv)	-644.5	-1272.8	-640.5
The peak height (Sp)	621.1	1562.2	621.1
The peak-valley height (Sy)	1205.5	2434.9	1325.5

From the table, the surface of the Al alloy is more smooth in the presence of the FBZ as a result of FBZ adsorption therefore the acid attack is reduced [42].

3.9. SEM test

Figure 11, suggests the micrograph given for Al alloy sheets in absence and using 300 ppm of FBZ after dipping for only one day.

From SEM image, the Al alloy surface is more degradation due to corrosion attack in the blank solution. The FBZ adsorption on the Al alloy surface, forming the shielding layer resulting in blocking the surface active areas so that the surface become more smooth and protection [43].

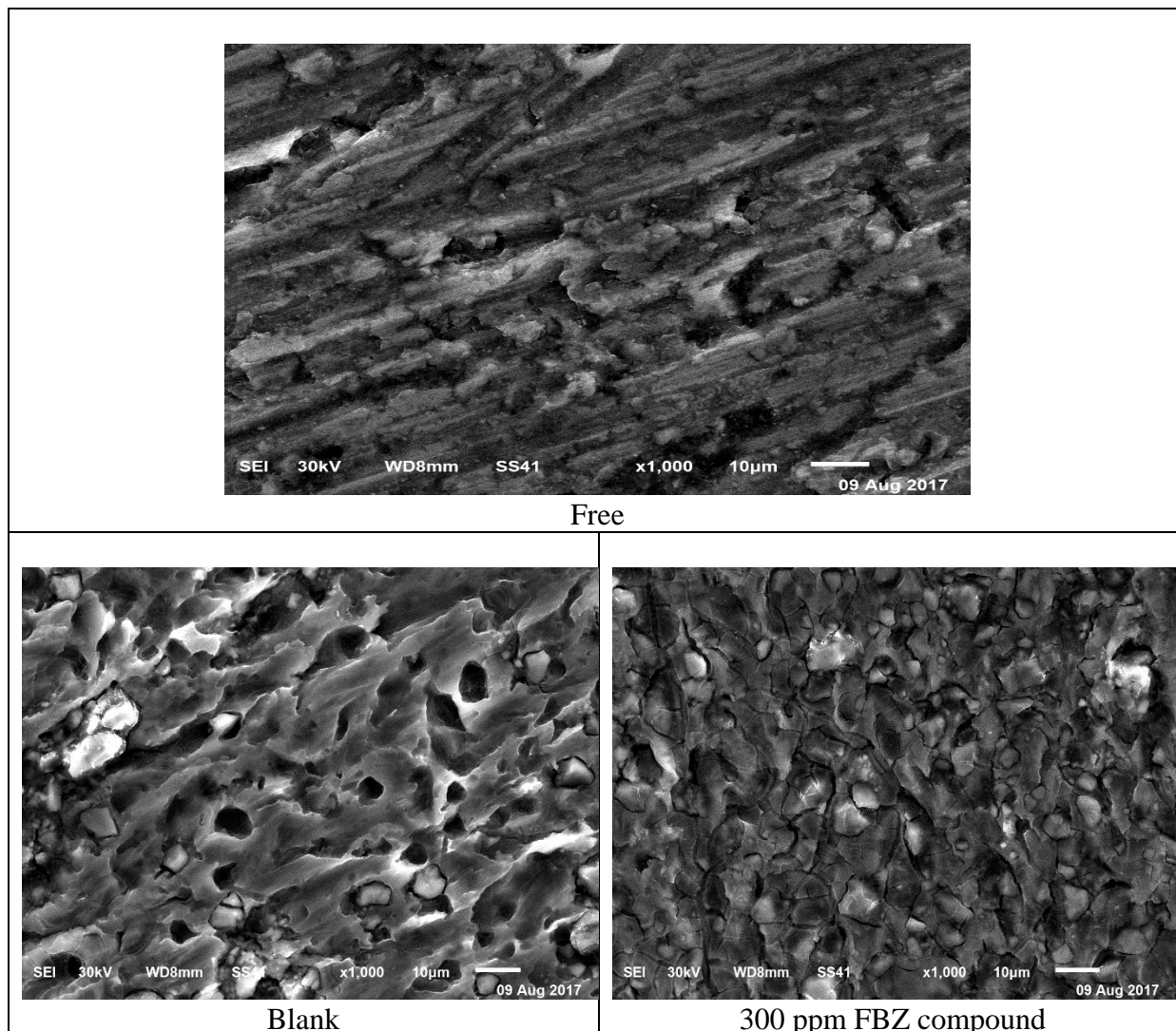


Figure11. SEM image for Al alloy with and without 300 ppm of study compound after immersion for 24 hours at 25°C

3.10. (FT – IR) analysis

FTIR were performed to confirm the adsorption of FBZ on aluminum surface. The FT-IR can be used to analyze the surface changes to prove the components nature which existed on the surface. The peak at 3306 cm^{-1} is corresponding to the stretching vibration of the amino group. This peak modified to 3356 cm^{-1} in the spectrum of the sample collected from the metal surface. Several peaks of FBZ in Figure 12 are modified / disappeared indicates the presence of chemical bonds between nitrogen and oxygen atoms of the FBZ to the metal surface and approve the presence of adsorbed FBZ film on the surface[44].

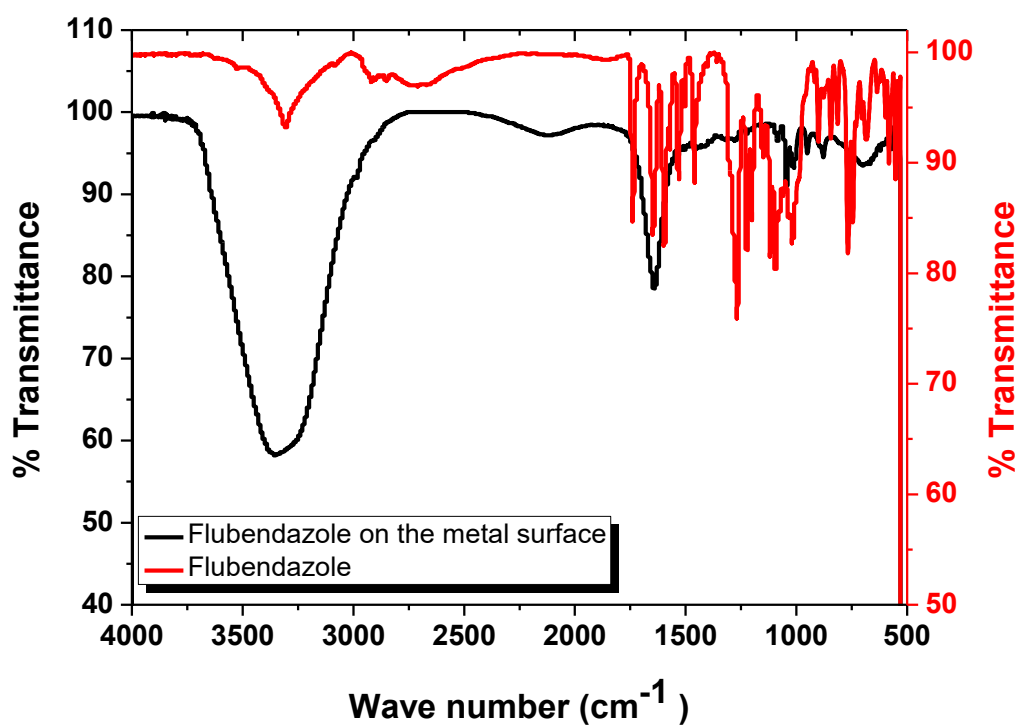


Figure 12. FT-IR spectra of FBZ solution (1000 ppm) (black spectrum line) and protective film of FBZ on Al alloy surface (the red spectrum line)

3.11. FBZ action mechanism

The Flubendazole action mechanism as a corrosion inhibitor for Al-Si alloy in 0.1 HCl has described by physical adsorption on the alloy surface. This proved from the values of $\Delta G_{\text{ads}}^{\circ}$ (less than 20 kJ mol^{-1}) and also from the effect of temperature (%IE decreases by raising temperature). This molecule (Flubendazole) will present in the protonated form, so it can adsorb directly on the negative surface of Al alloy [45] in acidic medium by electrostatic attraction as shown below

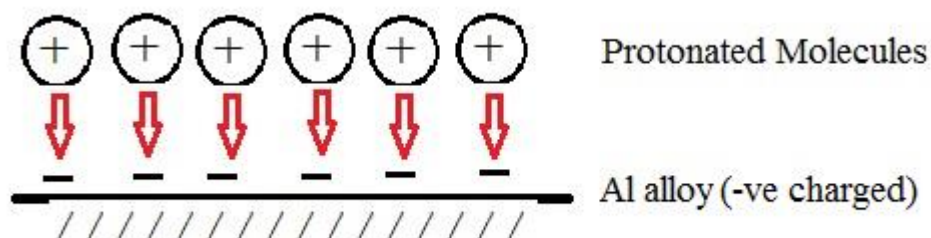


Table (10) gives a comparison of %IE with different investigated drugs. The present drug gives considerably significant corrosion %IE compared to other drugs. Thus, the present FBZ drug can be used as corrosion inhibitor with promising results.

Table 10. Performance comparison of some expired drugs as corrosion inhibitors

Inhibitor (drug)	sample	Medium	%IE	References
Penciillin G	mild steel	0.5 MH ₂ SO ₄	73.7	46
Domperidone	Al	0.2M HCl	89.1	47
Cloxacillin	mild steel	1 M HCl	81.0	48
Pantoprazole	Al	1M HCl	59.0	49
nizoral (NZR)	Al alloy	2M HCl	65.9	50
Quinoline	mild steel	1 M HCl	88.7	51
Penciillin V	mild steel	0.5 M H ₂ SO ₄	63.3	52
Flubendazole	Al-Si alloy	0.1M HCl	87.2	present work

4. CONCLUSIONS

The FBZ shows the corrosion inhibition for Al alloy in HCl solution, where IE ratio improved by rise of drug concentration. The IE is decreasing with rise of temperature as a result of the destruction of the adsorbed FBZ molecules on the Al alloy surface. The adsorption of Flubendazole on the surface follows Temkin equation. Tafel curves showed that FBZ is mixed-kind inhibitors. (C_{dl}) reduced by the rise of the FBZ concentration while (R_{ct}) is rise. The adsorbed layer on the Al alloy surface was proven by AFM, SEM and FTIR analyses.

References

1. R. S. Nathiya and V. Raj, *Egypt. J. Pet.*, 26 (2017) 313
2. S. L. Cohen, V. A. Brusica, F. B. Kaufman, G. S. Frankel, S. Motakef and B. Rush, *J. Vac. Sci. Technol. A.*, 8 (1990) 2417
3. E. E. Ebenso, N. O. Eddy and A. O. Odiongenyi, *Port. Electrochim. Acta.*, 27 (2009) 13
4. N. O. Eddy, E. E. Ebenso and U. J. Ibok, *J. Appl. Electrochem.*, 40 (2010) 445
5. N. O. Eddy, S. A. Odoemelam and A. J. Mbaba, *Afri. J. Pure Appl. Chem.*, 2 (2008) 132
6. N. O. Eddy and E. E. Ebenso, *Int. J. Electrochem. Sci.*, 5 (2010) 731
7. S.K. Shukla, A.K. Singh, I. Ahamad and M.A. Quraishi, *Mater. Lett.*, 63 (2009) 819
8. H. Ma, S. Chen, L. Niu, S. Zhao, S. Li and D. Li, *J. Appl. Electrochem.*, 32 (2002) 65
9. A. Samide, B. Tutunaru, C. Negrila, I. Trandafir and A. Maxut, *Dig. J. Nanomater. Bios.*, 6 (2011) 663
10. A. Samide, B. Tutunaru, C. Negrila and A. Dobritescu, *J. Therm. Anal. Calorim.*, 110 (2012) 145
11. T. Arslan, F. Kandemirli, E.E. Ebenso, I. Love and H. Alemu, *Corros. Sci.*, 51 (2009) 35
12. R. Solmaz, G. Kardas, B. Yazıcı and M. Erbil, *Prot. Met.*, 41 (2005) 628
13. A.S. Ekop and N.O. Eddy, *Aust. J. Basic Appl. Sci.*, 2 (2008) 1258
14. N.O. Eddy, S.A. Odoemelam and A.J. Mbaba, *Afr. J. Pure Appl. Chem.*, 2 (2008) 132
15. A.K. Singh and M.A. Quraishi, *Corros. Sci.*, 52 (2010) 152
16. A. Samide, *J. Environ. Sci. Health A Tox. Hazard. Subst. Environ. Eng.*, 48 (2013) 159
17. A.S. Fouda, H.A. Mostafa and H.M. El-Abbasy, *J. Appl. Electrochem.*, 40 (2010) 163
18. R.A. Prabhu, A.V. Shanbhag, T.V. Venkatesha, *J. Appl. Electrochem.*, 37 (2007) 491
19. S.K. Shukla and M.A. Quraishi, *Mater. Chem. Phys.*, 120 (2010) 142
20. I. Naqvi, A.R. Saleemi and S. Naveed, *Int. J. Electrochem. Sci.*, 6 (2011) 146

21. I. Ahamad and M.A. Quraishi, *Corros. Sci.*, 52 (2010) 651
22. S. K. Shukla, M.A. Quraishi and E.E. Ebenso, *Int. J. Electrochem. Sci.*, 6 (2011) 2912
23. X.H. Pang, W.J. Guo, W.H. Li, J.D. Xie and B.R. Hou, *Sci. China Ser. B-Chem.*, 51 (2008) 928
24. R. W. Bosch, J. Hubrecht, W. F. Bogaerts and B. C. Syrett, *Corrosion*, 57 (2001) 60.
25. S. S. Abdel-Rehim, K. F. Khaled and N. S. Abd-Elshafi, *Electrochim. Acta*, 51 (2006) 3269.
26. S. F. Mertens, C. Xhoffer, B. C. Decooman and E. Temmerman, *Corrosion*, 53 (1997) 381.
27. M. Lagrenée, B. Mernari, M. Bouanis, M. Traisnel and F. Bentiss, *Corros.Sci.*, 44 (2002) 573.
28. F. Bentiss, M. Lagrenée, and M. Traisnel, *Corrosion*, 56 (2000)733.
29. E. Kus and F. Mansfeld, *Corros. Sci.*, 48 (2006) 965.
30. D. Q. Zhang, Q. R. Cai, X. M. He, L. X. Gao, and G. S. Kim, *Mater. Chem. Phys.*, 114 (2009) 612.
31. G. TrabANELLI, in "Corrosion Mechanisms" (Ed. F. Mansfeld) Marcel Dekker, New York, (1987) 119.
32. A.S. Fouda, A. Abd El-Aal and A.B. Kandil, *Desalination*, 201 (2006) 216.
33. A. Fiala, A. Chibani, A. Darchen, A. Boulkamh and K. Djebbar, *Appl. Surf. Sci.*, 253(2007)9347.
34. W. Durnie, R.D. Marco, A. Jefferson and B. Kinsella, *J. Electrochem. Soc.*, 146 (1999) 1751.
35. M. K. Gomma and M. H. Wahdan, *Mater. Chem. Phys.*, 39 (1995) 209.
36. A. N. Frumkin, *Advances in electrochemistry and electrochemical engineering*, vol 3, chapter 5. Interscience Publisher Inc., New York, (1963)].
37. F. Bensajjay, S. Alehyen, M. El Achouri and S. Kertit, *Anti-Corros. Meth. Mater.*, 50 (2003) 402
38. L.Tang, X.Li, Y.Si, G.Mu and G.Liu, *Mater. Chem. Phys.*, 95 (2006) 29.
39. G.Mu, X. Li and G.Liu, *Corros. Sci.*, 47 (2005) 1932.
40. B. Wang, M. Du, J. Zang and C.J, Gao, *Corros.Sci.*, 53 (2011) 353.
41. S. Rajendran, C. Thangavelu and G. Annamalai, *J.Chem. Pharm.l Res.*, 4 (2012) 4836
42. A.S. Fouda, Y.M. Abdallah and D. Nabil, *IJIRSET*, 3 (2014) 12965
43. M. Abdallah, I. Zaafarany, S.O. Al-Karane and A.A. Abd El-Fattah , *Arabian Journal of Chemistry*, 5 (2012) 225
44. R.T. Morrison and Boyd's "Organic chemistry" 2nd ed., prentice-Hall of India, Pvt Ltd., New Delhi, 633, 1973.
45. M.N.Desai, *Werkst. U. Korros.*, 23 (1972) 475
46. H.Patmore, A.Jebreel, S.Uppal, C.H.Raine and P. Mc Whinney, *Am J Otolaryngol*, 31(5) (2010) 376
47. S.K. Rajappa, T. V. Venkatesh, *Int. J. Innov. Res.Sci. Eng.Technol.*, 5(3) (2016) 3917
48. S.H.Kumar and S.Karthikeyan, *J.Mater.EnvIRON.Sci.*, 3(5) (2012) 925
49. C.R. Jahromi and K. Dehghanian, *Int. J. Current Res.*,9(1) (2017) 44630
50. I.B. Obot and N.O. Obi-Egbedi, *E-Journal Chem.*, 7(3) (2010) 837
51. D.H. Kraus, S.J.Rehm and S.E.Kinney, *The Laryngoscope*, 98(9) (1988) 934.
52. G.J.Ridder, C.Breunig, J.Kaminsky and J.Pfeiffer, *Central skull base osteomyelitis: new insights and implications for diagnosis and treatment. European archives of oto-rhino-laryngology*, 272(5) (2015) 1269.